Available online at www.sciencedirect.com
ScienceDirect
Trans. Nonferrous Met. Soc. China 25(2015) 1968−1977
Transactions of Nonferrous Metals Society of China
www.tnmsc.cn

Effects of stoichiometric ratio La/Mg on structures and electrochemical performances of as-cast and annealed La−Mg−Ni-based A_2B_7-type electrode alloys

Yang-huan ZHANG[1,2], Tai YANG[2], Ting-ting ZHAI[2], Ze-ming YUAN[2], Guo-fang ZHANG[1], Shi-hai GUO[2]

1. Key Laboratory of Integrated Exploitation of Baiyun Obo Multi-metal Resources, Inner Mongolia University of Science and Technology, Baotou 014010, China;
2. Department of Functional Material Research, Central Iron and Steel Research Institute, Beijing 100081, China

Received 15 August 2014; accepted 29 October 2014

Abstract: In order to investigate the influences of the stoichiometric ratio of La/Mg (increasing La and decreasing Mg on the same mole ratio) on the structure and electrochemical performances of the La−Mg−Ni-based A_2B_7-type electrode alloy, the as-cast and the annealed ternary $La_{0.8+x}Mg_{0.2-x}Ni_{3.5}$ (x=0−0.05) electrode alloys were prepared. The characterization of electrode alloys by X-ray diffraction (XRD) and scanning electron microscopy (SEM) shows that all the as-cast and the annealed alloys hold two major phases of $(La,Mg)_2Ni_7$ and $LaNi_5$ as well as a residual phase of $LaNi_3$. Moreover, the increase of La/Mg ratio brings on a decline of $(La,Mg)_2Ni_7$ phase and a rise of $LaNi_5$ and $LaNi_3$ phases. The variation of La/Mg ratio gives rise to an evident change of the electrochemical performances of the alloys. The discharge capacities of the as-cast and the annealed alloys evidently decrease with growing the La/Mg ratio, while the cycle stabilities of the alloys visibly augment under the same condition. Furthermore, the high rate discharge ability (HRD), the electrochemical impedance spectrum (EIS), the Tafel polarization curves, and the potential step measurements all indicate that the electrochemical kinetic properties of the alloy electrodes increase with the La/Mg ratio rising.
Key words: hydrogen storage alloy; annealing treatment; structure; electrochemical performance; kinetics

1 Introduction

The discovery of rare earth-based AB_5-type hydrogen storage alloys makes the Ni−MH batteries commercialized in 1990. Consequently, the rare earth-based AB_5-type alloys have been industrialized on a large scale in China and Japan. With the development of the hydrogen storage electrode alloys, the application field of the Ni−MH is increasingly expanded. Particularly it is worth mentioning that the Ni/MH battery was considered to be one of the most promising candidates as the power sources for electric vehicles (EVs) [1]. As a matter of fact, hybrid electric vehicles (HEVs) with Ni−MH battery as the auxiliary power have been classified as mature products for nationwide selling by the Ministry of Industry and Information Technology of China, which provides a golden opportunity for the development of the Ni−MH battery. Some of the electrode alloys, involving the rare earth-based AB_5-type alloys [2,3], the AB_2-type Laves phase alloys [4], the V-based solid solution alloys [5] and the Mg-based alloys [6,7], are selected as potential electrode materials. However, none of which is qualified for the transport applications due to their limited properties, for example, the low discharge capacity for the AB_5-type alloy, the difficulty to be activated for the AB_2-type Laves phase as well as the V-based solid solution alloys, and the poor cycle stability for the Mg-based electrode alloy. Hence, the demand for new electrode materials with superior performances, especially higher discharge capacity, has become increasingly urgent. In view of this, La−Mg−Ni-based A_2B_7-type alloys have been deemed to be one of the most promising candidates as the negative electrode materials of Ni−MH battery on account of their higher discharge capacities (380−410 mA·h/g) and lower production costs, as reported by KADIR et al [8] and KOHNO et al [9]. However, this is seriously frustrated by their poor electrochemical cycle stability. Therefore, how to improve the cycle stability is still a main

Foundation item: Projects (51161015, 51371094) supported by the National Natural Science Foundation of China
Corresponding author: Yang-huan ZHANG; Tel: +86-10-62183115; Fax: +86-10-62187102; E-mail: zhangyh59@sina.com
DOI: 10.1016/S1003-6326(15)63805-5

challenge faced by researchers in this area.

It was found that the capacity deterioration of the La−Mg−Ni system alloy electrodes is mainly associated with the pulverization of the alloy particles and the oxidation/corrosion of the elements Mg and La during the electrochemical charge−discharge cycling [10−12]. Hence, it seems to be reasonable to believe that reducing the Mg content in the alloy will facilitate to improve the cycle stability of the alloy. Doubtlessly, the decrease of Mg content can result in some changes in the structures and the electrochemical performances of the alloys, so a deeper investigation is clearly necessary.

In this work, the as-cast and the annealed ternary La−Mg−Ni-based A_2B_7-type $La_{0.8+x}Mg_{0.2-x}Ni_{3.5}$ (x=0−0.05) alloys were prepared. The decreased amount of Mg is equal to the increased amount of La at the stoichiometric ratio of the alloys so as to keep the element content proportion of A-site and B-site the same (A: gross A-site elements, B: gross B-site elements). A systematic investigation about the effects caused by reducing the Mg content on the structures, morphologies and electrochemical properties of the experimental alloys was preformed.

2 Experimental

The purities of the raw materials of La, Mg and Ni can reach to 99.8% at least. The chemical compositions of the electrode alloys were $La_{0.8+x}Mg_{0.2-x}Ni_{3.5}$ (x=0, 0.01, 0.02, 0.03, 0.04 and 0.05), that is to say, the change of x representing the variation of La/Mg ratio. For convenience, the La/Mg ratio is donoted with the x value. The alloy ingots were prepared using a vacuum induction furnace in a helium atmosphere under the pressure of 0.04 MPa in order to prevent element Mg from volatilizing during the melting. A part of the alloys were annealed at 950 °C for 8 h in vacuum. Afterwards, the as-cast and the annealed alloys were crushed and mechanically ground to fine powders (passed through a 200-mesh sifter).

The phase structures and compositions of the alloys were characterized by X-ray diffraction (XRD) (D/max/2400). The diffraction, with the experimental parameters of 160 mA, 40 kV and 10 (°)/min, was performed with Cu K_α radiation filtered by graphite. The morphologies of the as-cast and the annealed alloys were examined by scanning electron microscopy (SEM) (QUANTA 400).

The round electrode pellets with a diameter of 15 mm were prepared by cold pressing the mixture of the alloy powder and carbonyl nickel powder with the mass ratio of 1:4 under the pressure of 35 MPa. Then the electrode pellets were immersed in 6 mol/L KOH solution for 24 h in order to wet the electrodes fully before the electrochemical measurement.

The electrochemical measurements were performed at 30 °C using a tri-electrode open cell, consisting of a working electrode (the metal hydride electrode), a sintered $Ni(OH)_2$/NiOOH counter electrode and a Hg/HgO reference electrode, which were immersed in the electrolyte of 6 mol/L KOH, and the voltage between the negative electrode and the reference one was defined as the discharge voltage. In every cycle, the alloy electrode was first charged with a constant current density. After resting for 15 min, it was discharged with the same current density to the cut-off voltage of −0.5 V.

To determine the electrochemical kinetics of the alloy electrodes, the EIS and the Tafel polarization curves of the alloys were measured at 30 °C using an electrochemical workstation (PARSTAT 2273). Prior to measuring the impedance and polarization curves, several electrochemical charging and discharging cycles were carried out in order to activate the materials. The fresh electrodes were fully charged and then rested for 2 h up to the stabilization of the open circuit potential. The EIS of the alloy electrodes was measured at 50% depth of discharge (DOD), the frequency was ranged from 10 kHz to 5 mHz, the amplitude of signal potentiostatic or galvanostatic measurements was 5 mV, the number of points per decade of frequencies was 60. The Tafel polarization curves were measured within the potential range of –1.2 to +1.0 V (vs Hg/HgO) at a scan rate of 5 mV/s. For the potentiostatic discharge, the test electrodes in the fully charged state were discharged at 500 mV potential steps for 5 ks on the electrochemical workstation (PARSTAT 2273) using the electrochemistry corrosion software (CorrWare).

3 Results and discussion

3.1 Influence of La/Mg ratio on structures of alloys

The phase components and structure characteristics of the as-cast and the annealed $La_{0.8+x}Mg_{0.2-x}Ni_{3.5}$ (x=0–0.05) alloys are detected by XRD analysis, just as shown in Fig. 1. The identification by means of international centre for diffraction data (ICDD) reveals that all the as-cast and the annealed alloys are of a multiphase structure, containing two major phases of $(La,Mg)_2Ni_7$ and $LaNi_5$ as well as a residual phase of $LaNi_3$. Evidently, the variation of La/Mg ratio and the annealing give rise to a clear change in the phase abundances instead of altering the phase composition. The lattice parameters together with the abundances of the three phases in the alloys which were calculated with Jade 6.0 software based on the XRD data are listed in Table 1. It is found that the rise of La/Mg ratio results in a clear increase of $LaNi_5$ and $LaNi_3$ phase while a decrease of $(La,Mg)_2Ni_7$ phase.

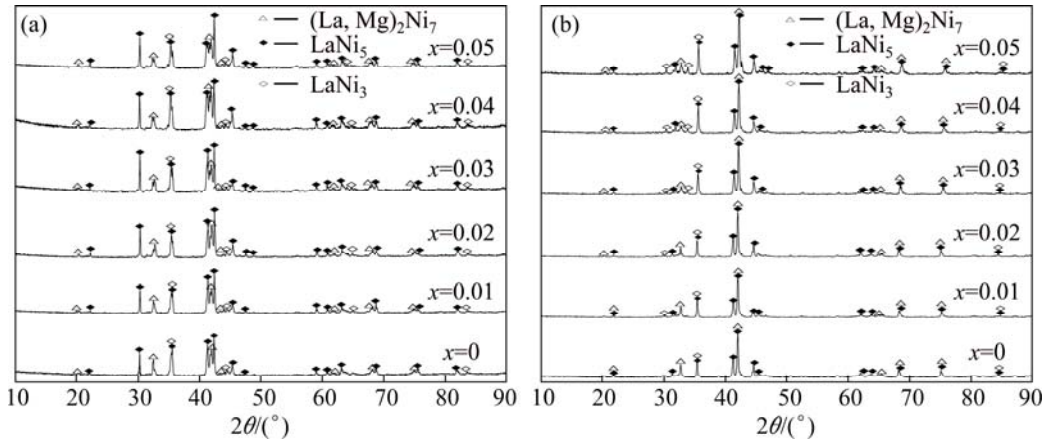

Fig. 1 XRD profiles of as-cast (a) and annealed (b) $La_{0.8+x}Mg_{0.2-x}Ni_{3.5}$ (x=0−0.05) electrode alloys

Table 1 Lattice parameters and abundances of three phases in alloys

Condition	La/Mg ratio	Major phase	Lattice constant		Cell volume/nm^3	Phase abundance (mass fraction)/%
			a/nm	c/nm		
As-cast	x=0	$(La, Mg)_2Ni_7$	0.50587	2.46431	0.5461	62.3
		$LaNi_5$	0.50533	0.38675	0.0855	25.5
		$LaNi_3$	0.50876	2.47109	0.5539	12.2
	x=0.01	$(La, Mg)_2Ni_7$	0.50589	2.46433	0.5462	60.2
		$LaNi_5$	0.50534	0.38677	0.0855	26.7
		$LaNi_3$	0.50577	2.47106	0.5474	13.1
	x=0.02	$(La, Mg)_2Ni_7$	0.50603	2.46441	0.5465	57.7
		$LaNi_5$	0.50537	0.38705	0.0856	28.4
		$LaNi_3$	0.50581	2.47109	0.5475	13.9
	x=0.03	$(La, Mg)_2Ni_7$	0.50605	2.46502	0.5467	54.8
		$LaNi_5$	0.50541	0.38741	0.0857	29.5
		$LaNi_3$	0.50602	2.47171	0.5481	15.7
	x=0.04	$(La, Mg)_2Ni_7$	0.50611	2.46508	0.5468	52.9
		$LaNi_5$	0.50563	0.38794	0.0859	30.1
		$LaNi_3$	0.50609	2.47182	0.5483	17.0
	x=0.05	$(La, Mg)_2Ni_7$	0.50618	2.46513	0.5470	51.6
		$LaNi_5$	0.50572	0.38805	0.0859	31.2
		$LaNi_3$	0.50615	2.47191	0.5484	17.2
As-annealed	x=0	$(La, Mg)_2Ni_7$	0.50602	2.46613	0.5469	70.3
		$LaNi_5$	0.50617	0.39025	0.0866	20.5
		$LaNi_3$	0.50881	2.47213	0.5542	9.2
	x=0.01	$(La, Mg)_2Ni_7$	0.50611	2.46625	0.5471	68.2
		$LaNi_5$	0.50619	0.39044	0.0866	21.7
		$LaNi_3$	0.50886	2.47218	0.5544	10.1
	x=0.02	$(La, Mg)_2Ni_7$	0.50615	2.46631	0.5472	65.6
		$LaNi_5$	0.50623	0.39049	0.0867	23.9
		$LaNi_3$	0.50894	2.47225	0.5546	10.5
	x=0.03	$(La, Mg)_2Ni_7$	0.50627	2.46652	0.5475	63.8
		$LaNi_5$	0.50658	0.39052	0.0868	25.1
		$LaNi_3$	0.50901	2.47272	0.5548	11.1
	x=0.04	$(La, Mg)_2Ni_7$	0.50631	2.46707	0.5477	59.2
		$LaNi_5$	0.50665	0.39079	0.0869	27.4
		$LaNi_3$	0.50913	2.47285	0.5551	13.4
	x=0.05	$(La, Mg)_2Ni_7$	0.50642	2.46711	0.5479	56.1
		$LaNi_5$	0.50672	0.39085	0.0869	28.4
		$LaNi_3$	0.50926	2.47301	0.5554	15.5

Moreover, the variation of La/Mg ratio has few effects on the lattice constants and the cell volumes of the alloys. It can be found from Table 1 that the annealing treatment makes the $(La,Mg)_2Ni_7$ phase visibly increase and the $LaNi_5$ phase as well as the $LaNi_3$ phase decrease. Meanwhile, the annealing treatment causes an obvious growth of lattice constants and cell volumes of the three phases in the alloy.

The SEM images and the energy dispersive spectrometer (EDS) patterns of the as-cast and the annealed $La_{0.8+x}Mg_{0.2-x}Ni_{3.5}$ (x=0−0.05) alloys are illustrated in Fig. 2. The EDS profiles reveal that all the experimental alloys hold a multiphase structure, containing phases of $(La, Mg)_2Ni_7$ and $LaNi_5$ as well as $LaNi_3$, which is consistent with the XRD examination. The morphologies of the as-cast alloys display a typical dendrite structure, which is hardly affected by the variation of La/Mg ratio. The annealing treatment gives rise to a significant variation which changes from the dendrite structure to the approximately equiaxial crystal. Meanwhile, the grains of the as-cast alloy are dramatically coarsened by the annealing.

3.2 Influence of La/Mg ratio on electrochemical performances

3.2.1 Activation capability and discharge capacity

Easy activation is indispensable for the alloy electrode applied in Ni−MH battery. The activation capability was evaluated by a number of charging−discharging cycles which are required for attaining the greatest discharge capacity at a constant current density. The variations of discharge capacities of the as-cast and the annealed $La_{0.8+x}Mg_{0.2-x}Ni_{3.5}$ (x=0−0.05) alloys with the cycle number are shown in Fig. 3. All the alloys demonstrate an excellent activation performance, attaining their maximum discharge capacities at most three charging−discharging cycles. Moreover, the growth of La/Mg ratio hardly impairs the activation capability of the as-cast and the annealed alloys. Based on the data in Fig. 3, the relationship between the discharge capacities and the La/Mg ratio of two states of the alloys can be established, as shown in Fig. 4. Apparently, the discharge

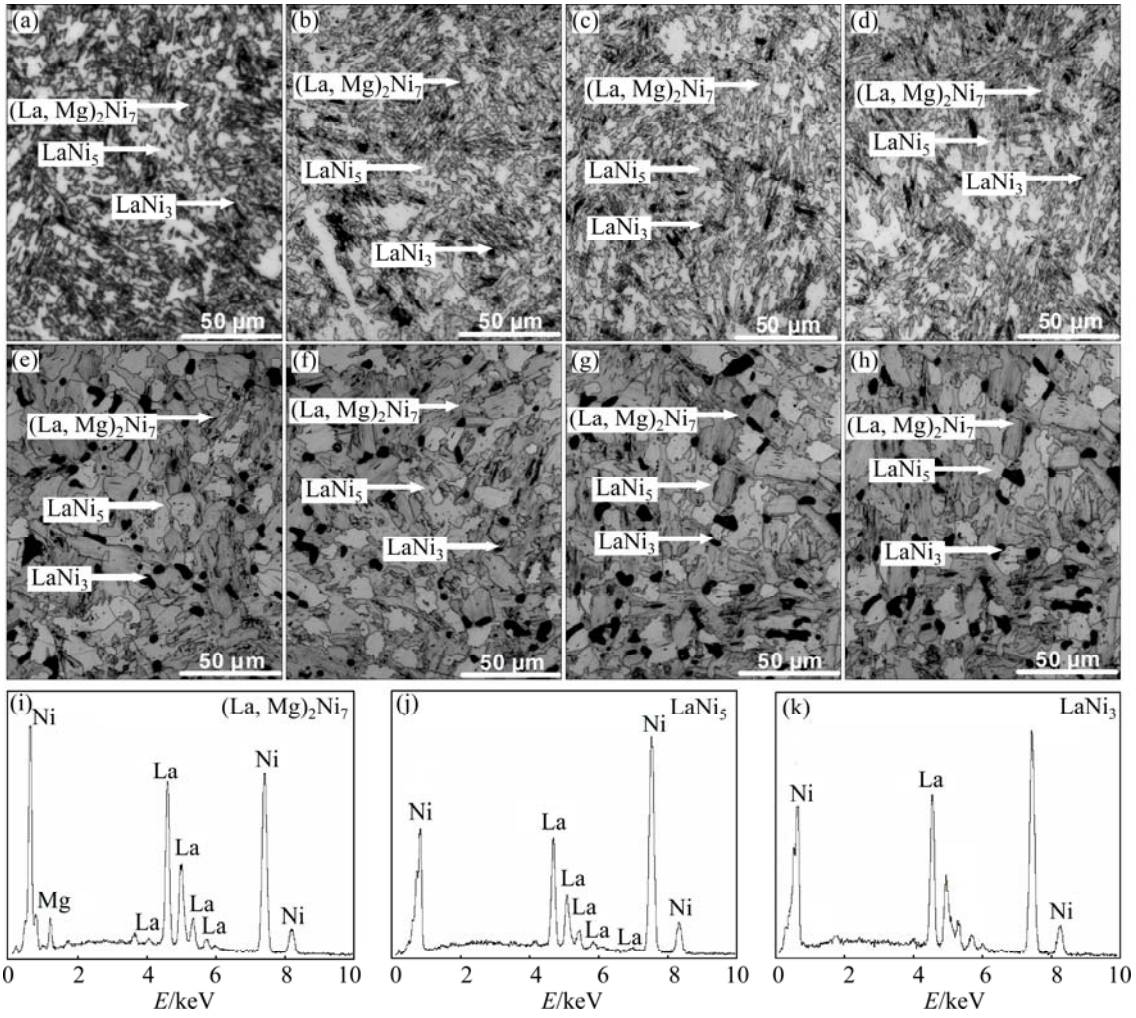

Fig. 2 SEM images (a−h) together with typical EDS spectra (i−k) of as-cast and annealed $La_{0.8+x}Mg_{0.2-x}Ni_{3.5}$ (x=0−0.05) electrode alloys: As-cast x=0 (a), 0.01 (b), 0.03 (c) and 0.05 (d); As-annealed x=0 (e), 0.01 (f), 0.03 (g) and 0.05 (h)

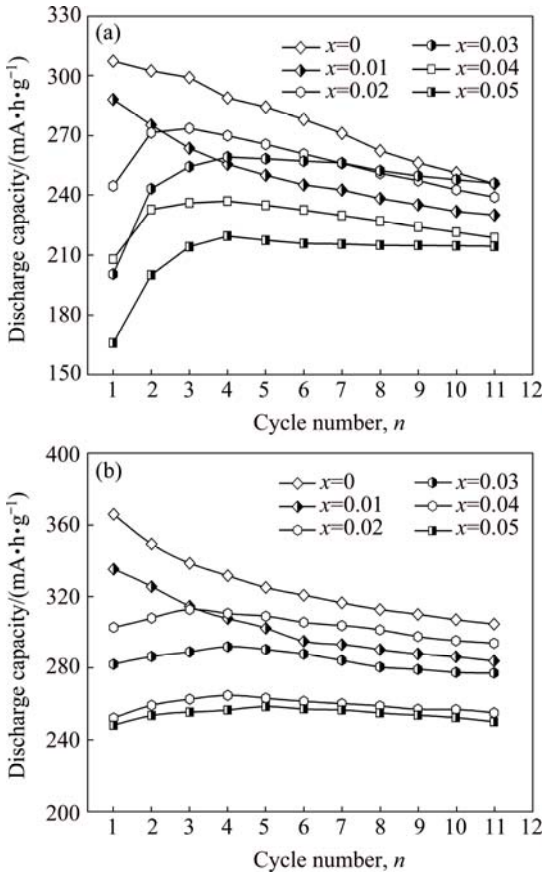

Fig. 3 Evolution of discharge capacity of as-cast (a) and annealed (b) $La_{0.8+x}Mg_{0.2-x}Ni_{3.5}$ (x=0−0.05) alloys with cycle number

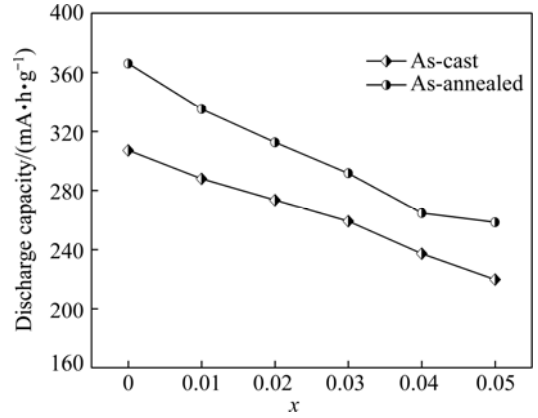

Fig. 4 Evolution of discharge capacity of as-cast and annealed $La_{0.8+x}Mg_{0.2-x}Ni_{3.5}$ (x=0−0.05) alloys with x value

capacities of the as-cast and the annealed alloys clearly decline with growing the La/Mg ratio. Specifically, increasing the La/Mg ratio from x=0 to x=0.05 makes the discharge capacities reduce from 307.2 to 219.7 mA·h/g for the as-cast alloy and from 366.0 to 258.5 mA·h/g for the as-annealed one. Furthermore, it is evident that, for all the La/Mg ratios, the as-annealed alloy exhibits much higher discharge capacities than the as-cast one, suggesting that the annealing treatment facilitates to improve the discharge capacity of the alloy. The annealing treatment makes the discharge capacity of the alloy considerably increase, which is attributed to the homogenization of the composition and the changes of the phase abundances as well as the lattice parameters originated by the annealing treatment.

It is believed that the superior activation performance of the as-cast and the annealed alloys is mainly ascribed to their multiphase structures. To sum up, the activation capability of the hydrogen storage alloy directly is associated with the change of the internal energy of the hydride system before and after absorbing hydrogen. The added internal energy comes from two aspects, which are the surface energy originating from the oxidation film on the surface of the electrode alloy, and the strain energy produced by the hydrogen atom entering into the interstitial sites of the tetrahedron or octahedron of the alloy lattice. The larger the added internal energy is, the poorer the activation performance of the alloy will be [13]. We all know that the phase boundary can decrease the lattice distortion and strain energy originated from the process of hydrogen absorption. Also, the phase boundary can provide good diffusion tunnels for the hydrogen atoms, enhancing the activation capability of the alloy. So, it can be concluded that the impaired activation capability by raising the La/Mg ratio can be ascribed to the increased amount of $LaNi_5$, as the activation ability of the $LaNi_5$ phase is a little lower than that of the $(La, Mg)_2Ni_7$ phase [10−12]. The reduced discharge capacity of the as-cast and the annealed alloys resulted from the La/Mg ratio growing is attributed to the increase of $LaNi_5$ and $LaNi_3$ phases, because their discharge capacities are much lower than those of the $(La, Mg)_2Ni_7$ phase.

3.2.2 Electrochemical cycle stability

The cyclic stability of hydrogen storage alloy, which is one of the major performance indicators that evaluate whether or not a kind of alloy can be applied as a negative electrode material, is characterized by the capacity retaining rate (S_n) which is defined as:

$$S_n=C_n/C_{max}\times100\% \quad (1)$$

where C_{max} is the maximum discharge capacity and C_n is the discharge capacity of the nth charge–discharge cycle at a current density of 300 mA/g. The variations of S_n values of the as-cast and the annealed $La_{0.8+x}Mg_{0.2-x}Ni_{3.5}$ (x=0−0.05) alloys with the cycle number are shown in Fig. 5, from which the degradation process of the discharge capacity of the alloys can be seen clearly. It is very evident that the slopes of curves substantially decline with rising the La/Mg ratio, suggesting that a higher La/Mg ratio is favor of the cycle stability of the alloy. In order to directly demonstrate the effects of the La/Mg ratio on the cycle stability of the as-cast and the

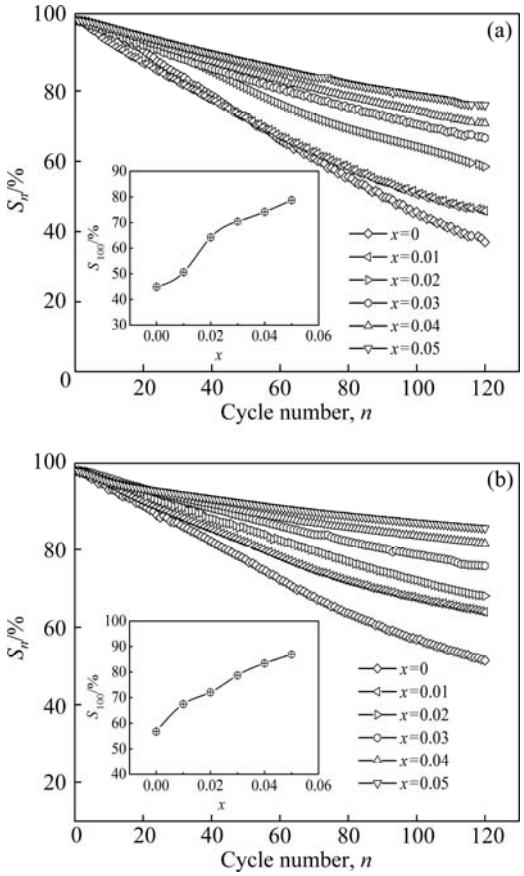

Fig. 5 Evolution of capacity retaining rates (S_n) of as-cast (a) and annealed (b) $La_{0.8+x}Mg_{0.2-x}Ni_{3.5}$ (x=0−0.05) alloys with cycle number

annealed alloy, the relationship between the S_{100} (n=100) values and the La/Mg ratio of the alloys is also inserted in Fig. 5. It is found that the S_{100} (n=100) values of the as-cast and the annealed alloys significantly grow with increasing the La/Mg ratio. More specifically, the S_{100} (n=100) values are enhanced from 44.9% to 78.8% for the as-cast alloy and from 56.8% to 86.9% for the as-annealed one by raising the La/Mg ratio from x=0 to x=0.05. It is worthy mentioning that the as-annealed alloy, for the same La/Mg ratio, exhibits clearly a higher S_{100} value than that of the as-cast one, meaning that the annealing treatment can improve the cycle stability of the alloy. Here, some elucidations are provided as the reasons why the increase of La/Mg ratio and the annealing treatment can ameliorate the cycle stability of the alloys. It is convinced that the following aspects are principally responsible for the fast degradation of the discharge capacity of La−Mg−Ni-based A_2B_7-type alloy during the charge−discharge cycling. Firstly, the constantly thickening surface layer of $Mg(OH)_2$ or $La(OH)_2$ hinders the hydrogen atoms from diffusing in or out of the alloys, in alkaline solution [14]. Moreover, an inevitable expansion and contraction of the cell volumes of the alloys during the charge−discharge process aggravates the cracking and pulverizing of the alloy and then makes the surface of the material apt to be oxidized, which was confirmed by the previous work [15]. The improved cycle stability of the as-cast and the annealed alloys by raising the La/Mg ratio is believed to be associated with the increase of $LaNi_5$ phase, due to an undoubted fact that the $LaNi_5$ phase possesses much higher electrochemical cycle stability than the $(La,Mg)_2Ni_7$ phase. As to the positive contribution of the annealing to the cycle stability of the alloys, it is ascribed to the increase of the cell volumes and more homogeneous compositional distribution generated by the annealing, which facilitates to restrain the pulverization and corrosion of the alloy [16,17].

3.2.3 Electrochemical kinetics

It is well known that with growing the current density, the discharge capacity of an electrode alloy will reduce in some degrees. However, keeping high discharge capacity during the charge−discharge cycles even with a high current density is important for the practical application of alloy electrode in Ni–MH battery, especially in power battery. Usually, the electrochemical kinetics of an alloy electrode is symbolized by its high rate discharge ability (HRD for short) which is defined as

$$HRD=C_J/C_{60}\times100\% \quad (2)$$

where C_J and C_{60} are the maximum discharge capacities of the alloy electrode charged−discharged at the current densities of J and 60 mA/g, respectively. The evolutions of HRD of the as-cast and the annealed $La_{0.8+x}Mg_{0.2-x}Ni_{3.5}$ (x=0–0.05) alloys with the discharge current density are shown in Fig. 6. Evidently, the variation of La/Mg ratio affects the HRD of the as-cast and the annealed alloys significantly. On the basis of the current density of 300 mA/g (J=300 mA/g), the relationships between the HRD of the as-cast and the annealed alloys and the La/Mg ratio are established, as inserted in Figs. 6(a) and (b), respectively. This indicates that the HRD values of all the alloys obviously augment with rising the La/Mg ratio. More specifically, the HRD is enhanced from 83.7% to 95.3% for the as-cast alloy and from 80.2% to 87.8% for the as-annealed one by increasing the La/Mg ratio from x=0 to x=0.05. Noticeably, the annealing treatment leads to a visible decline of HRD.

It is known that the high rate discharge ability of an alloy electrode basically depends on the charge-transfer rate on the alloy electrode surface and the hydrogen diffusion capability in the alloy bulk [18]. Hence, it seems to be compulsory to investigate the effects of the La/Mg ratio on the diffusion ability of hydrogen atoms and the charge-transfer rate, with the aim of discovering the mechanism that impacts the electrochemical kinetics of the alloy by varying the La/Mg ratio. The

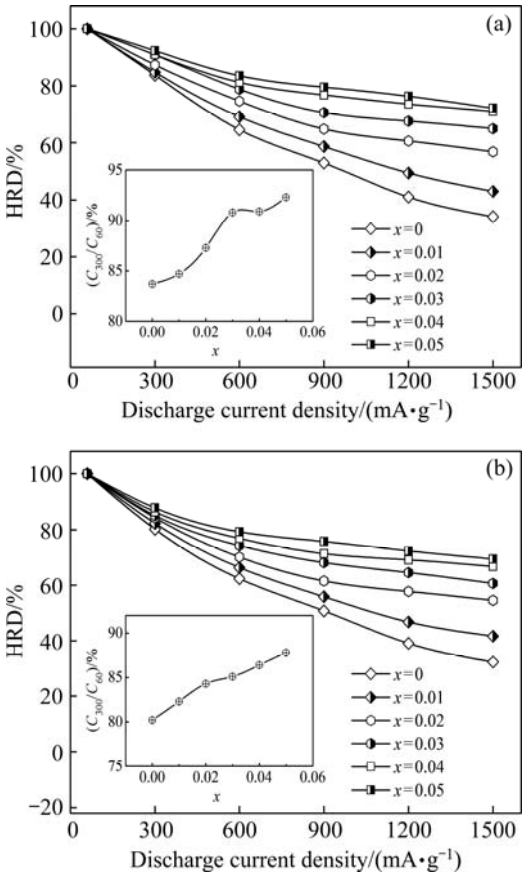

Fig. 6 Evolution of HRD of as-cast (a) and annealed (b) $La_{0.8+x}Mg_{0.2-x}Ni_{3.5}$ (x=0−0.05) alloys with discharge current density

hydrogen diffusion ability is evaluated by the hydrogen diffusion coefficient, which can be derived by means of the semilogarithmic curves of anodic current density versus working duration of an alloy electrode, as shown in Fig. 7. Based on the WHITE's model [19], the diffusion coefficient of the hydrogen atoms in the bulk of the alloy can be calculated by the slope of the linear region of the corresponding plots according to the following formulae:

$$\lg J_{\mathrm{d}} = \lg\left(\pm\frac{6FD}{da^2}(C_0 - C_{\mathrm{s}})\right) - \frac{\pi^2}{2.303}\frac{D}{a^2}t \tag{3}$$

$$D = -\frac{2.303a^2}{\pi^2}\frac{\mathrm{d}\lg J_{\mathrm{d}}}{\mathrm{d}t} \tag{4}$$

where J_{d} is the diffusion current density (A/g), D is the hydrogen diffusion coefficient (cm^2/s), C_0 is the initial hydrogen concentration in the bulk of the alloy (mol/cm^3), C_{s} is the hydrogen concentration on the surface of the alloy particles (mol/cm^3), a is the alloy particle radius (cm), d is the density of the hydrogen storage alloy (g/cm^3), and t is the discharge time (s). The evolutions of the D values of the as-cast and the annealed alloys obtained by Eq. (4) with the variation of La/Mg ratio are also inserted in Figs. 7(a) and (b), respectively, which indicate that the D values of the alloys clearly rise with the La/Mg ratio growing.

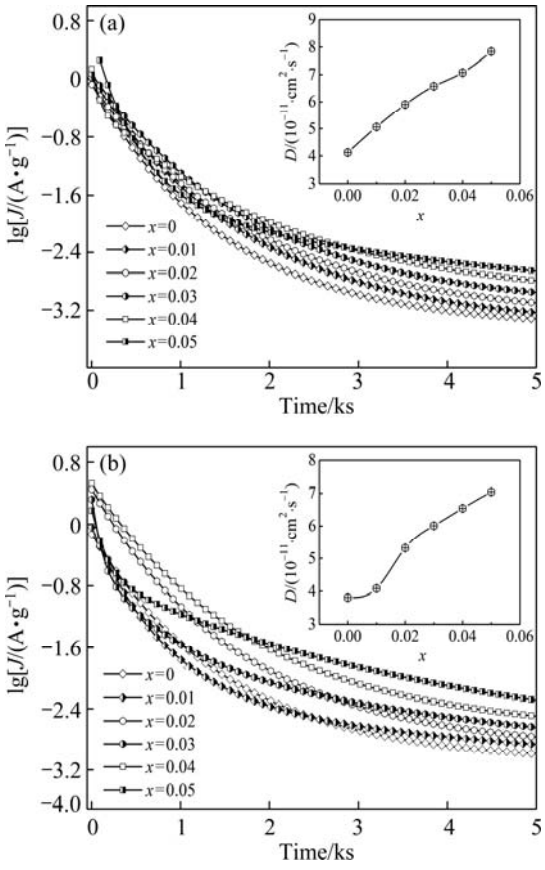

Fig. 7 Semilogarithmic curves of anodic current density vs time response of as-cast (a) and annealed (b) $La_{0.8+x}Mg_{0.2-x}Ni_{3.5}$ (x=0−0.05) alloys

Limiting current density (J_{L}), which is another important electrochemical kinetic parameter of an alloy electrode and is regarded to be related with the diffusion rate of hydrogen in the alloy electrode [20], can be obtained by measuring the Tafel polarization curve, as shown in Fig. 8. It is found that each anodic polarization curve shows an obvious inflection point, i.e., a critical value, which is called as J_{L}. It is indicated that an oxidation reaction takes place on the surface of the alloy electrode, and the oxidation layer hinders the hydrogen atoms from further penetrating [21]. Here, the J_{L} can be viewed as a critical current density for passivating. Based on the data in Fig. 8, the relationships between the J_{L} values and the La/Mg ratios of the as-cast and the annealed electrode alloys can be found, just as inserted in Figs. 8(a) and (b), respectively. The figures exhibit that the J_{L} values of the alloys evidently rise with increasing the La/Mg ratio. To be specific, raising the La/Mg ratio from x=0 to x=0.05 makes the J_{L} value increase from 0.927 to 1.917 A/g for the as-cast alloy and from 0.832 to 1.698 A/g for the annealed one.

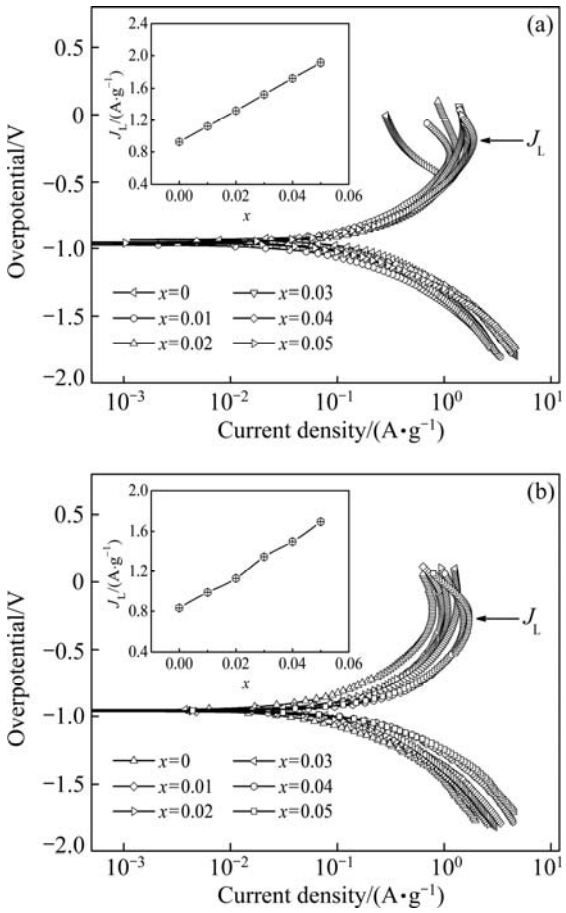

Fig. 8 Tafel polarization curves of as-cast (a) and annealed (b) $La_{0.8+x}Mg_{0.2-x}Ni_{3.5}$ (x=0−0.05) alloys

With regard to the charge-transfer capability, it can be qualitatively evaluated by the EIS based on the KURIYAMA's model [22]. The EIS of the as-cast and the annealed $La_{0.8+x}Mg_{0.2-x}Ni_{3.5}$ (x=0−0.05) alloys are provided in Fig. 9, from which it can be found out that each EIS has two distorted capacitive loops at high and middle frequencies separately as well as a line at low frequency, which very well express the electrochemical process of the alloy electrode. Among them, the smaller semicircle in the high frequency region is regarded to reflect the contact resistance between the alloy powder and the conductive material, and the larger one in the middle frequency region corresponds to the charge-transfer resistance on the alloy surface, while the straight line in low frequency represents the diffusion of hydrogenation in the alloy. In such cases, the charge-transfer capability can be estimated easily, namely the larger the radius of the semicircle in the middle frequency region is, the higher the charge-transfer resistance of the alloy electrode will be. It can be seen from Fig. 9 that the radii of the large semicircles of the as-cast and the annealed alloys in the middle frequency region markedly shrink with the La/Mg ratio growing, indicating that the increase of La/Mg ratio plays a significant positive contribution to the charge-transfer capability on the alloy electrode surface. Moreover, the radii of the large semicircles of the as-annealed alloy in middle frequency are larger than those of the as-cast one. This means that the annealing treatment decreases the charge-transfer capability on the alloy electrode surface.

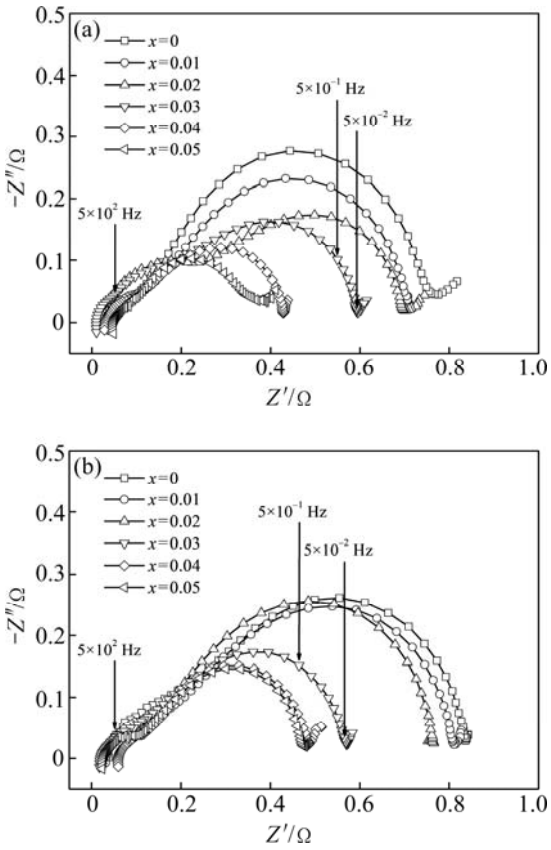

Fig. 9 Electrochemical impedance spectra (EIS) of as-cast (a) and annealed (b) $La_{0.8+x}Mg_{0.2-x}Ni_{3.5}$ (x=0−0.05) alloys

Based on the above-mentioned results, some acceptable elucidations can be provided as the reasons why increasing the La/Mg ratio brings about a positive contribution to the HRD and the electrochemical kinetics of the alloys. The electrochemical hydriding/dehydriding reaction can be described as follows:

$$M+xH_2O+xe \rightleftharpoons MH_x+xOH^- \quad (5)$$

where M is the hydrogen storage alloy. The hydrogen atom attaching to the surface of the alloy electrode is suggested to have two possible whereabouts, combining together to form hydrogen molecule or producing metal hydride via diffusion. This means that the utilization of charging current, depending on the diffusion rate of hydrogen atom within the surface layer of alloy, is just the ratio of the diffusion current to the imposed current. Equation (5) indicates that when the alloy electrode is charged in KOH solution, hydrogen atoms on the alloy−electrolyte interface diffuse into bulk alloy and

then store themselves in the metallic lattice in the form of hydride. In the process of discharging, the hydrogen stored in the bulk alloy diffuses toward the alloy electrode surface where it is oxidized. Hence, it can be concluded that the electrochemical hydrogen storage kinetics of the alloy electrode is controlled by the charge-transfer rate on the surface of the alloy electrode and the hydrogen diffusion capability in the alloy bulk. Thus, it is believed that the enhanced capabilities of the diffusion of hydrogen atom and the charge-transfer by raising the La/Mg ratio are the direct causes that increase the HRD values of the as-cast and the annealed alloys. As to the enhanced hydrogen diffusion and charge-transfer rate, it should be ascribed to the increased amount of $LaNi_5$ phase generated by the La/Mg ratio rising because the $LaNi_5$ phase possesses better electro-catalytic activation than that of the $(La, Mg)_2Ni_7$ phase. The annealing treatment changes the structure of the alloy, therefore causes a decreased HRD, detailedly described as follows: the annealing treatment eliminates the internal strain of casting and diminishes crystalline defects such as dislocations and grain boundaries, thus not only increases the charge-transfer resistance of the alloy electrode but also hinders the diffusion of hydrogen from the inner of the bulk to the surface, and subsequently aggravates the decline of electrochemical kinetic property.

4 Conclusions

1) The ternary La−Mg−Ni-based A_2B_7-type $La_{0.8+x}Mg_{0.2-x}Ni_{3.5}$ (x=0−0.05) electrode alloys were successfully fabricated by casting and annealing. All the alloys contain two major phases of $(La, Mg)_2Ni_7$ and $LaNi_5$ as well as a residual phase of $LaNi_3$. The increase of La/Mg ratio gives rise to an increase of $LaNi_5$ and $LaNi_3$ phases and a decrease of $(La, Mg)_2Ni_7$ phase clearly instead of altering the phase structure of the alloys.

2) The variation of La/Mg ratio engenders an evident influence on the electrochemical performances of the alloys. Specifically, the rise of La/Mg ratio results in a significant reduction of discharge capacity of the as-cast and the annealed alloys while improves the cycle stability and the HRD, for which the changed phase abundances of the alloys introduced by varying the La/Mg ratio are chiefly responsible.

3) Furthermore, the annealing treatment brings on an obvious impact on the structure and the electrochemical characteristics of the alloys. In particular, it not only enhances the discharge capacity and cycle stability of the alloys dramatically, but also leads to a decline of HRD values of the alloys.

References

[1] SAKINTUNA B, LAMARI-DARKRIM F, HIRSCHER M. Metal hydride materials for solid hydrogen storage: A review [J]. International Journal of Hydrogen Energy, 2007, 32(9): 1121−1140.

[2] WILLEMS J J G, BUSCHOW K H J. From permanent magnets to rechargeable hydride electrodes [J]. Journal of the Less Common Metals, 1987, 129(15): 13−30.

[3] WEI Fan-song, LI Li, XIANG Hong-fu, LI Hui, WEI Fan-na. Phase structure and electrochemical properties of $La_{1.7+x}Mg_{1.3-x}(NiCoMn)_{9.3}$ (x=0−0.4) hydrogen storage alloys [J]. Transactions of Nonferrous Metals Society of China, 2012, 22(8): 1995−1999.

[4] OVSHINSKY S R, FETCENKO M A, ROSS J. A nickel metal hydride battery for electric vehicles [J]. Science, 1993, 260(5105): 176−181.

[5] TSUKAHARA M, KAMIYA T, TAKAHASHI K, KAWABATA A, SAKURAI S, SHI J, TAKESHITA HT, KURIYAMA N, SAKAI T. Hydrogen storage and electrode properties of V-based solid solution type alloys prepared by a thermic process [J]. Journal of the Electrochemical Society, 2000, 147(8): 2941−2944.

[6] SONG Wen-jie, LI Jin-shan, ZHANG Tie-bang, HOU Xiao-jiang, KOU Hong-chao, XUE Xiang-yi, HU Rui. Microstructure and hydrogenation kinetics of Mg_2Ni-based alloys with addition of Nd, Zn and Ti [J]. Transactions of Nonferrous Metals Society of China, 2013, 23(12): 3677−3684.

[7] ZHANG Yang-huan, YANG Tai, BU Wen-gang, CAI Ying, ZHANG Guo-fang, ZHAO Dong-liang. Effect of Nd content on electrochemical performances of nanocrystalline and amorphous $(Mg_{24}Ni_{10}Cu_2)_{100-x}Nd_x$ (x=0−20) alloys prepared by melt spinning [J]. Transactions of Nonferrous Metals Society of China, 2013, 23(12): 3668−3676.

[8] KADIR K, SAKAI T, UEHARA I. Synthesis and structure determination of a new series of hydrogen storage alloys; RMg_2Ni_9 (R=La, Ce, Pr, Nd, Sm and Gd) built from $MgNi_2$ Laves-type layers alternating with AB_5 layers [J]. Journal of Alloys and Compounds, 1997, 257(1−2): 115−121.

[9] KOHNO T, YOSHIDA H, KAWASHIMA F, INABA T, SAKAI I, YAMAMOTO M. Hydrogen storage properties of new ternary system alloys: La_2MgNi_9, $La_5Mg_2Ni_{23}$, $La_3Mg_2Ni_{14}$ [J]. Journal of Alloys and Compounds, 2000, 311(2): L5−L7.

[10] ZHANG Yang-huan, REN Hui-ping, CAI Ying, YANG Tai, ZHANG Guo-fang, ZHAO Dong-liang. Structures and electrochemical hydrogen storage performance of Si added A_2B_7-type alloy electrodes [J]. Transactions of Nonferrous Metals Society of China, 2014, 24(2): 406−414.

[11] ZHANG Yang-huan, HOU Zhong-hui, YANG Tai, ZHANG Guo-fang, LI Xia, ZHAO Dong-liang. Structure and electrochemical hydrogen storage characteristics of $La_{0.8-x}Pr_xMg_{0.2}Ni_{3.15}Co_{0.2}Al_{0.1}Si_{0.05}$ (x=0−0.4) electrode alloys [J]. Journal of Central South University of Technology, 2013, 20(5): 1142−1150.

[12] ZHANG Yang-huan, HOU Zhong-hui, LI Bao-wei, REN Hui-ping, CAI Ying, ZHAO Dong-liang. Electrochemical hydrogen storage characteristics of as-cast and annealed $La_{0.8-x}Nd_xMg_{0.2}Ni_{3.15}Co_{0.2}Al_{0.1}Si_{0.05}$ (x=0−0.4) alloys [J]. Transactions of Nonferrous Metals Society of China, 2013, 23(5): 1403−1412.

[13] WU M S, WU H R, WANG Y Y, WAN C C. Surface treatment for hydrogen storage alloy of nickel/metal hydride battery [J]. Journal of Alloys and Compounds, 2000, 302(1−2): 248−257.

[14] DORNHEIM M, DOPPIU S, BARKHORDARIAN G, BOESENBERG U, KLASSEN T, GUTFLEISCH O, BORMANN R. Hydrogen storage in magnesium-based hydrides and hydride composites [J]. Scripta Materialia, 2007, 56(10): 841−846.

[15] ZHANG Y H, LI C, CAI Y, HU F, LIU Z H, GUO S H. Highly improved electrochemical hydrogen storage performances of the Nd–Cu-added Mg_2Ni-type alloys by melt spinning [J]. Journal of Alloys and Compounds, 2014, 584: 81−86.

[16] LIU Y F, PAN H G, GAO M X, WANG Q D. Advanced hydrogen storage alloys for Ni/MH rechargeable batteries [J]. Journal of Materials Chemistry, 2011, 21(13): 4743−4755.

[17] LIU Y F, CAO Y H, HUANG L, GAO M X, PAN H G. Rare earth–Mg−Ni-based hydrogen storage alloys as negative electrode materials for Ni/MH batteries [J]. Journal of Alloys and Compounds, 2011, 509(3): 675−686.

[18] PAN H G, CHEN N, GAO M X, LI R, LEI Y Q, WANG Q D. Effects of annealing temperature on structure and the electrochemical properties of $La_{0.7}Mg_{0.3}Ni_{2.45}Co_{0.75}Mn_{0.1}Al_{0.2}$ hydrogen storage alloy [J]. Journal of Alloys and Compounds, 2005, 397(1−2): 306−312.

[19] ZHENG G, POPOV B N, WHITE R E. Electrochemical determination of the diffusion coefficient of hydrogen through an $LaNi_{4.25}Al_{0.75}$ electrode in alkaline aqueous solution [J]. Journal of the Electrochemical Society, 1995, 142(8): 2695−2698.

[20] RATNAKUMAR B V, BOWMAN R C, HIGHTOWER A, FULTZ B, WITHAM C. Electrochemical studies on $LaNi_{5-x}Sn_x$ metal hydride alloys [J]. Journal of the Electrochemical Society, 1996, 143(8): 2578−2584.

[21] ZHAO X Y, DING Y, MA L Q, WANG L Y, YANG M, SHEN X D. Electrochemical properties of $MmNi_{3.8}Co_{0.75}Mn_{0.4}Al_{0.2}$ hydrogen storage alloy modified with nanocrystalline nickel [J]. International Journal of Hydrogen Energy, 2008, 33(22): 6727−6733.

[22] KURIYAMA N, SAKAI T, MIYAMURA H, UEHARA I, ISHIKAWA H, IWASAKI T. Electrochemical impedance and deterioration behavior of metal hydride electrodes [J]. Journal of Alloys and Compounds, 1993, 202(1−2): 183−197.

化学计量比 La/Mg 对铸态及退火态 La–Mg–Ni 系 A_2B_7 型电极合金结构及电化学性能的影响

张羊换[1,2]，杨 泰[2]，翟亭亭[2]，袁泽明[2]，张国芳[1]，郭世海[2]

1. 内蒙古科技大学 内蒙古自治区白云鄂博矿多金属资源综合利用重点实验室，包头 014010；
2. 钢铁研究总院 功能材料研究所，北京 100081

摘 要：采用合金熔炼及退火处理的方法制备 La−Mg−Ni 系 A_2B_7 型 $La_{0.8+x}Mg_{0.2-x}Ni_{3.5}$ (x=0−0.05)电极合金，并研究不同的化学计量比 La/Mg 对该合金的相结构和电化学性能的影响。通过 X 射线衍射(XRD)和扫描电子显微镜(SEM)对合金进行表征。结果表明：合金包含$(La, Mg)_2Ni_7$和 $LaNi_5$两个主相以及一些残余相 $LaNi_3$。随着 La/Mg 比率的增大，合金中的$(La, Mg)_2Ni_7$相含量降低，而 $LaNi_5$和 $LaNi_3$相的含量升高。La/Mg 比的变化也使得合金电极的电化学性能发生显著变化。随着 La/Mg 比率的增加，铸态及退火态合金的放电容量降低，而循环稳定性明显改善。此外，合金电极的高倍率放电性能(HRD)、电化学阻抗谱(EIS)、Tafel 极化曲线以及电势阶跃的测量均表明 La/Mg 比率的增加提高了合金的电化学动力学性能。

关键词：贮氢合金；退火处理；相结构；电化学性能；动力学

(Edited by Mu-lan QIN)